*Original Article*

# The effect of recombinant chimeric swine PKR-Apaf-1 proteins on viral-load reduction of PRRS and PED alpha-coronavirus infected cell lines

**Phong Vu Anh Tuan Vo[1] Thanaporn Lertsakchai[1] Sukeesom Jiramahasuwan[1]**

**Achara Tawatsin[1] Athipoo Nuntaprasert[1*]**

## *Abstract*

The PRRS virus and PED alpha-coronavirus are the two main pig pathogens in the world. The current strategies to control these diseases are inadequate. The recombinant chimeric swine PKR-Apaf-1 protein (rcPAP) consists of the Human Immunodeficiency Virus Trans-activator transcription (HIV-TAT) domain, the dsRNA-binding domain of porcine Protein kinase R (PKR) gene and the caspase recruitment domain (CARD) domain of porcine Apoptotic Protease-Activating Factor-1 (Apaf-1) gene. In general, the rcPAP can detect viral dsRNA in virally infected cells and induces apoptosis and kills the virus-infected cells. In this study, the reducing viral-load efficacy of rcPAP (produced from bacteria) against PRRS virrus and PED alpha-coronavirus replication in the cell line was studied. The four concentrations of rcPAP (40, 60, 80 and 120 µg/ml) were studied at three different periods (24, 36 and 48 h post inoculation (hpi)). The results showed that no cytotoxicity in two cell lines was observed during rcPAP addition. The rcPAP (80 µg/ml) significantly increased the monkey active caspase-3 levels at 17.09 for the PRRS virus and at 15.96-fold for the PED alpha-coronavirus at 48 hpi, respectively ($p < 0.05$). The viral RNA copy numbers at 48 hpi were significantly reduced up to 84.47% of PRRS virus and up to 82.98% for PED alpha-coronavirus when treated with rcPAP (80 µg/ml) ($p < 0.05$), respectively. Interestingly, the viral titers at 48 hpi were dramatically decreased by 87.76% for PRRS virus and by 86.29% for PED alpha-coronavirus in virus-infected cells treated with rcPAP (80 µg/ml), respectively. The results also demonstrated that the rcPAP was able to reduce the viral load and viral N protein synthesis in both virus-infected cell lines. In conclusion, the results suggest that rcPAP is likely to be a valuable therapeutic agent against both PRRS virus and PED alpha-coronavirus infection.

**Keywords:** Antiviral activity, apoptosis, cytotoxicity, PRRS virus, PED alpha-coronavirus

[1]*Faculty of Veterinary Science, Chulalongkorn University, Henri-Dunant Rd., Pathumwan, Bangkok 10330, Thailand*
****Correspondence**: Athipoo.N@chula.ac.th* (A. Nuntaprasert)
Received January 14, 2021
Accepted November 21, 2021
https://doi.org/10.14456/tjvm.2022.10

## Introduction

The Porcine reproductive and respiratory syndrome (PRRS) virus and Porcine epidemic diarrhea (PED) alpha-coronavirus are two major pathogens infecting pigs around the world (Lee 2015, OIE 2015). The current control strategies have been shown to limit the impact of these diseases. The limited numbers of available antivirals reflect the difficulty of developing therapeutics to treat viral diseases, both at a practical and financial level (Pozzo and Thiry 2014). As obligate intracellular parasites, the replication of the virus is intricately linked to normal cell processes and thus many compounds such as antiviral drugs that interfere with viral replication are inherently toxic to host cells and present a low therapeutic index (Quinn *et al*., 2015). Moreover, there is evidence about new variant strains of some swine viruses (Song *et al*., 2015) that are resistant to antiviral drugs and may become more powerful super-viruses (Rider *et al*., 2011). Therefore, new effective strategies to control swine viral diseases is urgently needed and will likely require utilizing the latest technologies and evolving practices enhancing their disease-fighting powers in order to eventually eradicate those viruses.

The ideal therapeutically safe and effective antiviral molecules will selectively affect specific processes of the target virus with minimal side effects on normal cellular pathways. There are many reports about antiviral activity against viral diseases in swine. Firstly, the RNA interference has been reported as antiviral drugs which target the viral genome or viral receptors (Choi *et al*., 2009, Abba *et al*., 2015, Li *et al*., 2015, Liwei *et al*., 2015). Secondly, plant extract compounds have been found to inhibit viral replication or viral infection or directly destroy the viral particles (Abba *et al*., 2015). Thirdly, recombinant proteins could be used as antivirals (Rider *et al*., 2011, Zhang *et al*., 2013, Guo *et al*., 2015, Mojtaba Sharti *et al*., 2021) since they can induce apoptosis and kill viral-infected cells. However, an effective strategy to control swine viral diseases is still limited.

One of the novel options would be to use swine viral-specific and efficacious antiviral activity like a rcPAP. The rcPAP has been successfully produced from the bacterial system according to the human DRACO concept (Vo *et al*., 2020). The recombinant chimeric swine PKR-Apaf-1 protein (rcPAP) consists of the Human Immunodeficiency Virus Trans-activator transcription (HIV-TAT) domain, the dsRNA-binding domain of porcine Protein kinase R (PKR) gene and the caspase recruitment domain (CARD) domain of porcine Apoptotic Protease-Activating Factor-1 (Apaf-1) gene. In general, the rcPAP can detect viral dsRNA in virally infected cells via the dsRBD of swine PKR. After two or more rcPAP molecule crosslinks on the same viral dsRNA, the rcPAP induces apoptosis and kills the virus-infected cells. As an alternative approach to induce apoptosis in viral infected cells and to reduce viral mRNA expression or translation, the rcPAP molecule produced from bacteria was carried out to study the *in vitro* effect against the PRRS virus and PED alpha-coronavirus.

## Materials and Methods

***Cell culture, rcPAP, and virus:*** MARC-145 (ATCC: CRL-12231) (Ma *et al*., 2013) and Vero (ATCC: CRL-1587) (Borel *et al*., 2010) cell lines were cultured in Dulbecco's modified Eagle's medium (DMEM) supplemented with 10% fetal bovine serum (FBS) and maintained at 37 °C in 5% $CO_2$ incubator. The rcPAP was cloned and expressed using pET-His6-TEV-LIC plasmid. HiTrap chelating affinity column (HiTrap™ Chelating HP, Germany) was used to purify rcPAP. The rcPAP was dialyzed against PBS overnight using the Cellu-Sep® T2 Tubings dialysis membrane (Membrane Filtration Products, USA) and the purification of rcPAP confirmed using Western blot analysis. The rcPAP concentration was measured on the Bradford assay using the Bicinchoninic Acid (BCA) protein Assay Kit (Thermo Fisher Scientific, USA). The rcPAP (stock at 1 mg/ml) was used at a series of four concentrations of 40, 60, 80 and 120 µg/ml). US strain PRRS virus (Thai isolates 01NP01, stock virus at 6 log10 ($TCID_{50}$/ml)), PED alpha-coronavirus (Thai isolates 01CB01, stock virus at 6 log10 ($TCID_{50}$/ml)) were used in this study. PRRS virus was propagated in MARC-145 cells while the PED alpha-coronavirus was propagated in Vero cells.

***Cytotoxicity assay:*** The cytotoxicity of rcPAP was evaluated using MTT assay in two types of cell line including MARC-145 cells and Vero cells in six independent experiments. Each experiment involved triplicate wells per concentration. MACR-145 cells or Vero cells were detached using 0.5% Trypsin/EDTA (Invitrogen, USA), re-suspended in complete medium and then dispensed into 96-well plates at a density of $10^4$ cells per well. After incubation for 24 h, the rcPAP were administered to the wells at varying final concentrations (40, 60, 80, and 120 µg/ml) (Guo *et al*., 2015) and incubated at 37 °C, in a humidified 5% $CO_2$ incubator for 48 h. Then, 10 µl of MTT reagent (5 mg/ml) (Dojindo, Japan) was added to each well (Ding *et al*., 2005) and incubated for 4 h to allow the conversion of MTT to formazan crystals by mitochondrial dehydrogenase, prior to the addition of 100 µl of 10% (v/v) SDS in 50% (v/v) N, N-dimethylformamide (Merck, USA) to solubilize the formazan crystals without removing the medium (Uma *et al*., 2008). An ELISA plate reader (Multiskan EX, Thermo Scientific, USA) was used to record the absorbance at 570 nm. The percentage of cell viability was calculated using equation (Valiyari *et al*., 2012):

% Cell Viability = 100 - % Cytotoxicity (% Cytotoxicity = 1-(mean absorbance of treated cells/mean absorbance of negative control)).

The cytotoxic effect of rcPAP on two types of cells (as above) was also determined by the Trypan blue viability assay (Billack *et al*., 2008). Cells ($10^4$ per well) in 24 well-plates were cultured at varying final concentrations of rcPAP (as shown above) for 48 h. Then, the adherent and non-adherent cells were brought into suspension using 0.5% Trypsin/EDTA (Invitrogen, USA). The cell suspension was centrifuged at 150 g for 5 mins and the cells were washed with PBS. DMEM supplement with 10% FBS and 0.5% Trypan blue (Merck, USA) was used to resuspended cells and

incubated for 5 mins. Then, a 20 µL aliquot was removed and placed on a Neubauer hemocytometer (Precicolor, Germany). Finally, the numbers of viable and nonviable cells were counted under a microscope. The percent viability was calculated as follows:

Cell viability (%) = (viable cells/ the total cell count) × 100

***Cell transduction assays of rcPAP:*** For determination of protein transduction efficiency, the rcPAP internalization was assessed by Western blot analysis (Rider *et al*., 2011, Zhang *et al*., 2013). Either MARC-145 cells or Vero cells in 6-well plates were cultured in DMEM with rcPAP at a concentration of 40, 60, 80 and 120 µg/ml (Zhang *et al*., 2013, Vo *et al*., 2020) for varying times (up to 5 h) and then cells were trypsinized and washed thoroughly with PBS to remove any rcPAP on the cell surface. Lysates from approximately $10^5$ cells were added to the well. A known amount of purified rcPAP was used as a standard as indicated. The rcPAP were identified using western blotting with mouse anti-6x His monoclonal antibodies (1: 1,000 dilution) (GenScript, USA) and goat anti-mouse IgG HRP (1: 2,000 dilution) (GenScript, USA).

To test rcPAP persistence inside the cells, four concentrations of rcPAP (as shown above) (Zhang *et al*., 2013) were administered to the culture medium and incubated for 5 h (Zhang *et al*., 2013), and then the cells were washed with PBS and put into the medium without rcPAP. The cells were collected every 12 h (up to 48 h) and analyzed as described above.

***Reducing viral-load activity of the rcPAP:*** The antiviral assay was performed in six independent experiments. For PRRS virus (Wernike *et al*., 2012), the MARC-145 cells were seeded in a 6-well plate at a density of $10^5$ cells per well and cultured for 24 h at 37 °C, in a 5% $CO_2$ incubator. Then the cells were inoculated with Thai isolated US strain PRRS virus at a 200 $TCID_{50}$ per well for 6 h at 37 °C, and the viral inoculum was then removed and the cell monolayer was washed with PBS. For PED alpha-coronavirus (Choi *et al*., 2009), the antiviral assay followed the above procedure with a 400 $TCID_{50}$ per well and the virus was inoculated 1 h before the rcPAP administration. The various concentrations of rcPAP (40, 60, 80 and 120 µg/ml) (Guo *et al*., 2015) with the fresh medium were added. One positive control (cell line inoculated with viruses only) and two negative controls (one cell line with medium only and another with rcPAP) were included. The cells were cultured for 24 hpi; 36 hpi or 48 hpi after each rcPAP administration to medium at 37 °C, in a 5% $CO_2$ incubator, the supernatants were collected for virus yield titration and the cell monolayer was washed three times with PBS. The qantitative real-time RT-PCR (qRT-PCR) were tested the viral RNA in either culture cells or supernatants at different times post-inoculation. Viral titers in the culture supernatants were determined and calculated as log10 ($TCID_{50}$/ml). The monkey active caspase-3 levels (a key protease activated during early stages of apoptosis) in cultured cells were determined using ELISA analysis (Wardi *et al*., 2014). Western blot technique was used to detect nucleocapsid (N) protein synthesis of the PRRS virus and the PED alpha-coronavirus in culture cells.

***Quantitative Real-time RT-PCR (qRT-PCR):*** The qRT-PCR was used to detect and quantify the RNA copy of PRRS virus and PED alpha-coronavirus based on ORF7 gene of the PRRS virus (Wernike *et al*., 2012, Guo *et al*., 2015) and on the spike (S) gene of PED alpha-coronavirus (Miller *et al*., 2016). The pCR2.1-ORF7-US plasmid for PRRS virus or pCR2.1-S plasmid for PED alpha-coronavirus were constructed using a pCR2.1®TA cloning kit (Invitrogen, USA) according to the manufacturer's instruction. Viral RNA was extracted from either culture cells or supernatants. The procedure of total RNA isolation was performed following the protocol of the commercial kit's instruction (PureLink™ Viral RNA/DNA Kit, Invitrogen, USA). Then, RNA concentration was measured (using Nanodrop ND-2000, Thermo Scientific, USA), diluted to equal concentration and reverse-transcribed onto cDNA using Superscript® III Reverse Transcriptase (Invitrogen, USA). The generated cDNA was amplified by qRT-PCR using the following specific primers as shown in Table 1. The qRT-PCR was developed for the detection of each virus using SYBR Green I fluorescent dye using Thunderbird®Sybr®qPCR Mix (Toyobo, Japan). The qRT-PCR reaction was performed using the ABI 7300 System (Applied Biosystems, USA) in 96-well plates. The cycling conditions are shown in Table 2. The qRT-PCR was performed in triplicate using 10-fold serial dilutions of the pCR2.1-ORF7-US plasmid for PRRS virus or the pCR2.1-S plasmid for PED alpha-coronavirus, with a concentration ranging from 10 to 10 log10 (copies/ml) as standard. Positive (cells infected virus without rcPAP) and two negative (one cell only and other cells plus rcPAP) controls were tested along with the unknown samples.

**Table 1** Nucleotide sequences of the primers used for qRT-PCR

| Gene | Sense | Sequence (5′ to 3′) | GenBank accession number | Product size (bp) | Reference |
|---|---|---|---|---|---|
| ORF7 of PPRS virus US strain | + | GCAATTGTGTCTGTCGTC | **GU454850** | 81 | (Wernike *et al*., 2012) |
| | - | CTTATCCTCCCTGAATCTGAC | | | |
| Spike gene of PED alpha-coronavirus | + | ACGTCCCTTTACTTTCAATTCACA | **KF272920** | 111 | (Miller *et al*., 2016) |
| | - | TATACTTGGTACACACATCCAGA GTCA | | | |

**Table 2** The qRT-PCR condition program

| cDNA | | ORF7 of PRRS virus US strain | Spike gene of PED alpha-coronavirus |
|---|---|---|---|
| 1 cycle | Denaturation | 95 °C (1 min) | 95 °C (1 min) |
| 40 cycles | Denaturation | 95 °C (1 min) | 95 °C (1 min) |
| | Annealing | 57 °C (15 sec) | 59 °C (15 sec) |
| | Extension (data collection) | 72 °C (45 sec) | 72 °C (45 sec) |

***Viral Titration:*** Viral titers in culture supernatants of each pathogen (PRRS virus and PED alpha-coronavirus) were determined by log10 ($TCID_{50}$/ml). Briefly, cells were seeded into 96-well culture plates at a density of $10^4$ cells per well and then incubated for 24 h to reach at least 80 % confluence before infection. The viral culture supernatants were serially diluted10-fold, from $10^{-1}$ to $10^{-9}$ dilutions and 200 µl of each dilution were put into each of six wells. Each cell line was maintained by medium free virus serving as a control. The cells were incubated at 37 °C in an incubator containing 5% $CO_2$ for 48 hpi. An inverted microscope was used for a daily check of cell cytopathic effect (CPE) for PRRS virus and PED alpha-coronavirus (Lee 2015) but IPMA technique (Tatsanakit *et al*., 2003) was used to determine PRRS virus titers. The PRRS virus nucleocapsid protein antibody (GTX129270, GeneTex, USA) was used. The log10 ($TCID_{50}$/ml) was calculated using the Reed–Muench method (Reed and Muench 1938).

***Western blot analysis:*** The N protein of PRRS virus or PED alpha-coronavirus was performed using Western blot analysis as described elsewhere (Guo *et al*., 2015). Briefly, the lysates from the rcPAP treated either PRRS virus-infected MARC-145 cells or PED alpha-coronavirus infected Vero cells were separated by SDS-PAGE (12.5% (w/v) resolving gel) and then transferred to a polyvinyl difluoride (PVDF) membrane (Pall Corporation, USA) in transfer buffer (20 mM Tris-HCl, 192 mM glycine, 0.1% (w/v) SDS, 20% (v/v) methanol, pH 8.3) using a semi-dry transfer unit (Amersham, USA) for 1.5 h. The membrane was blocked with 5% (w/v) skimmed milk in PBS at 4 °C overnight and then incubated with 1: 2,000 dilution of anti-PRRS virus N monoclonal antibodies (Rural Technologies, USA) or with 1: 2,000 dilution of PED alpha-coronavirus N monoclonal antibodies (Medgene Labs, USA) at 37 °C for 1 h, washed three times in PBS/0.5% (v/v) Tween 20 (PBS-T), and then incubated with 1: 2,000 dilution of horseradish peroxidase (HRP)-conjugated goat anti-mouse IgG (Sigma, USA) at 37 °C for 1 h. After washing (as above), the color was developed by incubation with the 3, 3-diaminobenzidine (Dojindo, Japan) for 15–30 mins and the color development was terminated by rinsing with distilled water.

***Apoptosis assay:*** Monkey active caspase-3 (which cleaved at Asp175/Ser176) from lysates of monkey cell lines was detected and quantified (Wardi *et al*., 2014) using the Monkey Active caspase-3 ELISA Kit (MyBioSource, USA) in 96-well plates under the manufacturer's instruction. After treating cells with rcPAP, floated and adherent cells (MARC-145 cells and Vero cells) were pelleted and washed in cold PBS and lysed with cell extraction buffer (Invitrogen, USA) (10 mM Tris, pH 7.4, 100 mM NaCl, 1 mM EDTA, 1 mM EGTA, 1 mM NaF, 20 mM $Na_4P_2O_7$, 2 mM $Na_3VO_4$, 1% Triton X-100, 10% glycerol, 0.1% SDS, 0.5% deoxycholate) and 1 mM PMSF and protease inhibitor cocktail (Invitrogen, USA). The lysates were centrifuged at 13,000 rpm for 10 mins at 4 °C. The protein concentration of the cell extract supernatants was determined as the total protein using a BCA protein assay kit (Pierce, USA) with bovine serum albumin (BSA) at 25–2,000 µg/ml as the reference standards. The cell extract supernatants were then used to determine the concentration of monkey active caspase-3 levels (Wardi *et al*., 2014). The OD (optical density) of this colored product was measured at 450 nm with an ELISA Reader (Multiskan EX, Thermo Scientific, USA) and this OD is directly proportional to the concentration of monkey active caspase-3 present in the sample. The results (ng/mg protein) represented as monkey active caspase-3 levels (ng) per protein concentration of cell extract supernatants (mg).

***Statistics analysis:*** All data was presented as means ± standard deviation (SD) from six independent experiments. Each experiment involved triplicate wells per concentration. Statistical analysis was performed by analysis of variance (ANOVA) (F test). A $p < 0.05$ was considered statistically significant.

## *Results*

***Cell viability:*** The cytotoxicity of the rcPAP was determined using MTT and Trypan blue assays as shown in MARC-145 cells (Fig. 1A) and in Vero cells (Fig. 1B), respectively. The rcPAP treated both cell lines showed no cytotoxicity from 40 µg/ml to a concentration of 80 µg/ml (100% of cell viability) using either MTT or Trypan blue assays. However, the rcPAP showed cytotoxicity at a concentration of 120 µg/ml. The percentage of cell viability using MTT assay was decreased 1.13 ± 0.12% on Vero cells and 1.54 ± 0.28% of MARC-145 cells and using Trypan blue assay was decreased 3.62 ± 0.06% on Vero cells and 4.36 ± 0.09% of MARC-145 cells.

***Cell transduction assay of rcPAP:*** The rcPAP (35 kDa protein band) transduction in MARC-145 cells and Vero cells was demonstrated by Western blot analysis. Four concentrations of rcPAP (40, 60, 80 and 120 µg/ml) were examined for penetration and persistence on both cell lines. We found that the time of the rcPAP existing and persisting inside both cells responded in a dose independent manner (data not shown). According to the reduction of percent cell viability of both cells treated with rcPAP at a concentration of 120 µg/ml, our design was intended to observe the effect of rcPAP at the 80 µg/ml. As shown in Fig. 2 and Fig. 3, the rcPAP was detected using the Western blot technique in each cell line which was treated with an

80 µg/ml of rcPAP. The results indicated that the rcPAP began to enter into each cell line within 1 h and was still detected in both MARC-145 cells and Vero cells for a period of at least 48 h.

***Reducing viral-load activity of the rcPAP***

***PRRS virus-infected MARC-145 cells:*** The qRT-PCR results showed that the rcPAP (40, 60, 80 and 120 µg/ml) significantly reduced PRRS RNA virus numbers in a dose-dependent manner between rcPAP-treated and untreated PRRS virus-infected MARC-145 cells at three different periods (24, 36 and 48 h post inoculation (hpi)) ($p$ <0.05) as shown in Figs. 4A and B. As expected, the viral RNA numbers of two negative controls were undetermined in both culture cells and supernatants during the study. At 24 hpi, the highest reduction of viral RNA numbers in rcPAP-treated PRRS virus-infected cells (80 µg/ml) were 23.13% (4.46 ± 0.005 vs 5.84 ± 0.008 log10 (copies/ml)) in culture cells and 23.76% (4.17 ± 0.005 vs 5.47 ± 0.001 log10 (copies/ml)) in culture supernatants compared with those of untreated MARC-145 cells ($p$ < 0.05). At 36 hpi following rcPAP (80 µg/ml) treated PRRS virus-infected MARC-145 cells, mean PRRS viral RNA numbers (the highest reduction) were 43.18% (3.67 ± 0.001 vs 6.46 ± 0.001 log10 (copies/ml)) in culture cells and 46.50% (3.21 ± 0.003 vs 6.00 ± 0.008 log10 (copies/ml)) in culture supernatants compared with those of untreated MARC-145 cells ($p$ < 0.05). Interestingly, the rcPAP (80 µg/ml) treated PRRS virus-infected MARC-145 cells significantly decreased the viral RNA numbers with the highest reduction by 75.55% (1.75 ± 0.008 vs 7.16 ± 0.009 log10 (copies/ml)) and 84.47% (1.02 ± 0.002 vs 6.57 ± 0.002 log10 (copies/ml)) in culture cells and supernatants, respectively, at 48 hpi ($p$ < 0.05). These results clearly showed that the highest reduction of viral RNA numbers was found at a concentration of 80 µg/ml of rcPAP treated PRRS virus-infected MARC-145 cells when taking pictures under the inverted microscope shown in Figs. 5A (without rcPAP) and B (with rcPAP). These results illustrated that the rcPAP may have an antiviral activity in vitro.

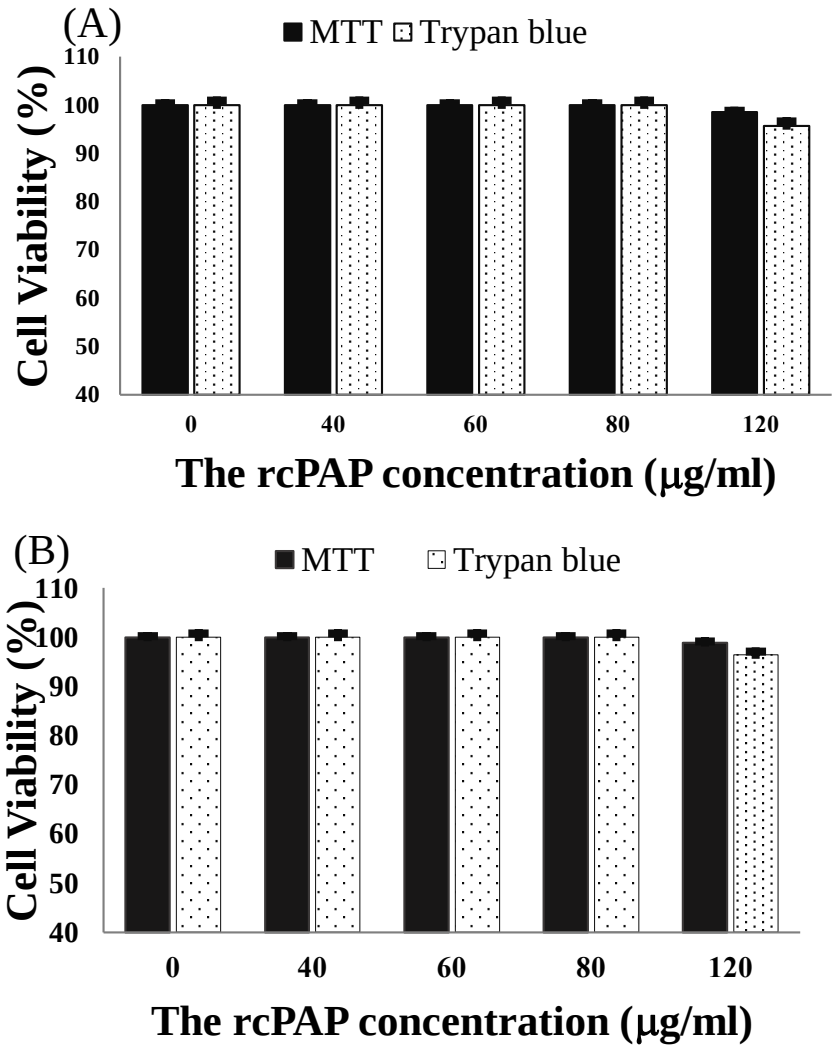


**Figure 1** The cytotoxicity of the rcPAP in (A) MARC-145 cells and (B) Vero cells was measured using MTT and Trypan blue assay. Data is shown as mean ± SD of six independent experiments. Bars represent the standard deviation.

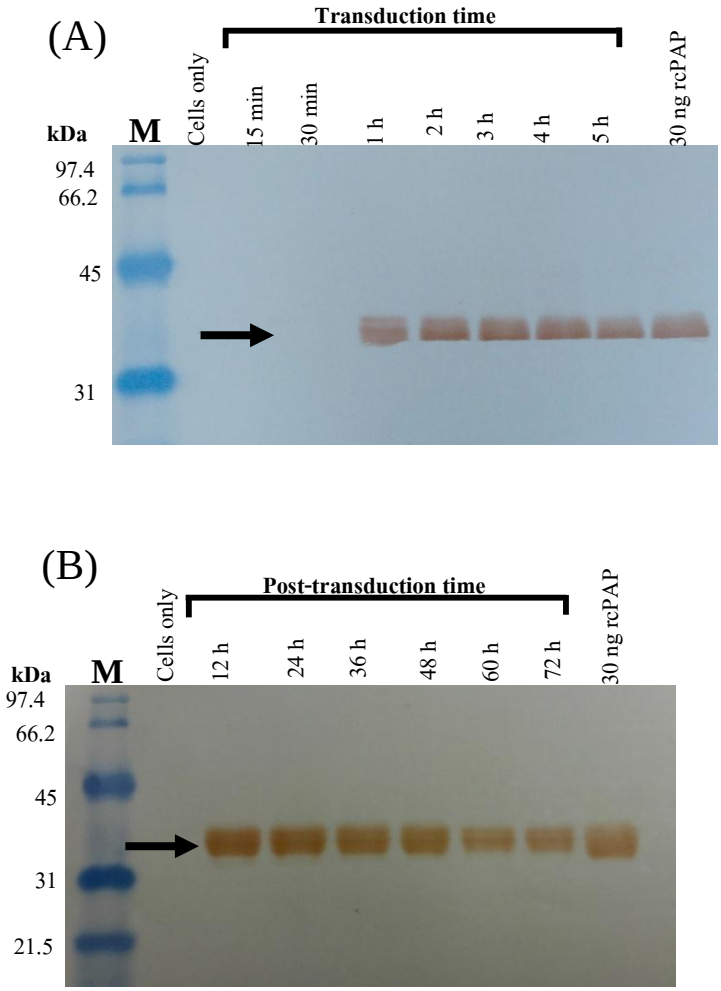


**Figure 2** The band of rcPAP (80 mg/ml) transduced cells persisting for days in MARC-145 cells. The Western blot analysis of (A) transduction and (B) persistence of rcPAP. M, Protein markers (kDa); Protein markers (BioRad) are indicated in kilodalton (kDa).

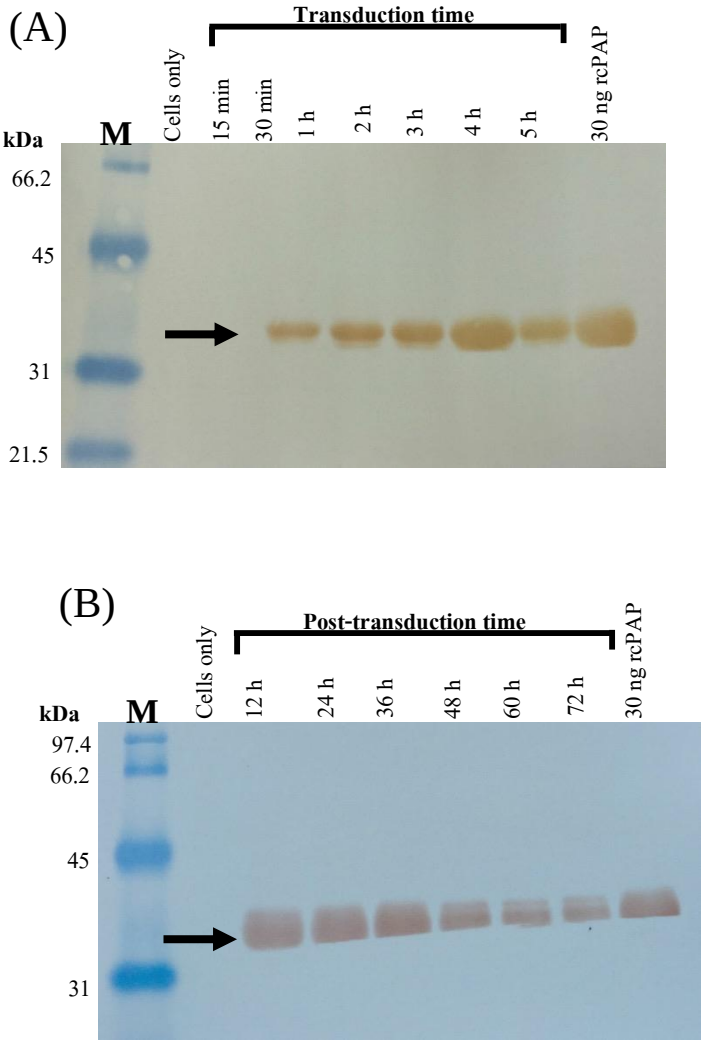


**Figure 3** The band of rcPAP (80 mg/ml) transduced cells persisting for days in Vero cells. The Western blot analysis of (A) transduction and (B) persistence of rcPAP. M, Protein markers; Protein markers (BioRad) are indicated in kDa.

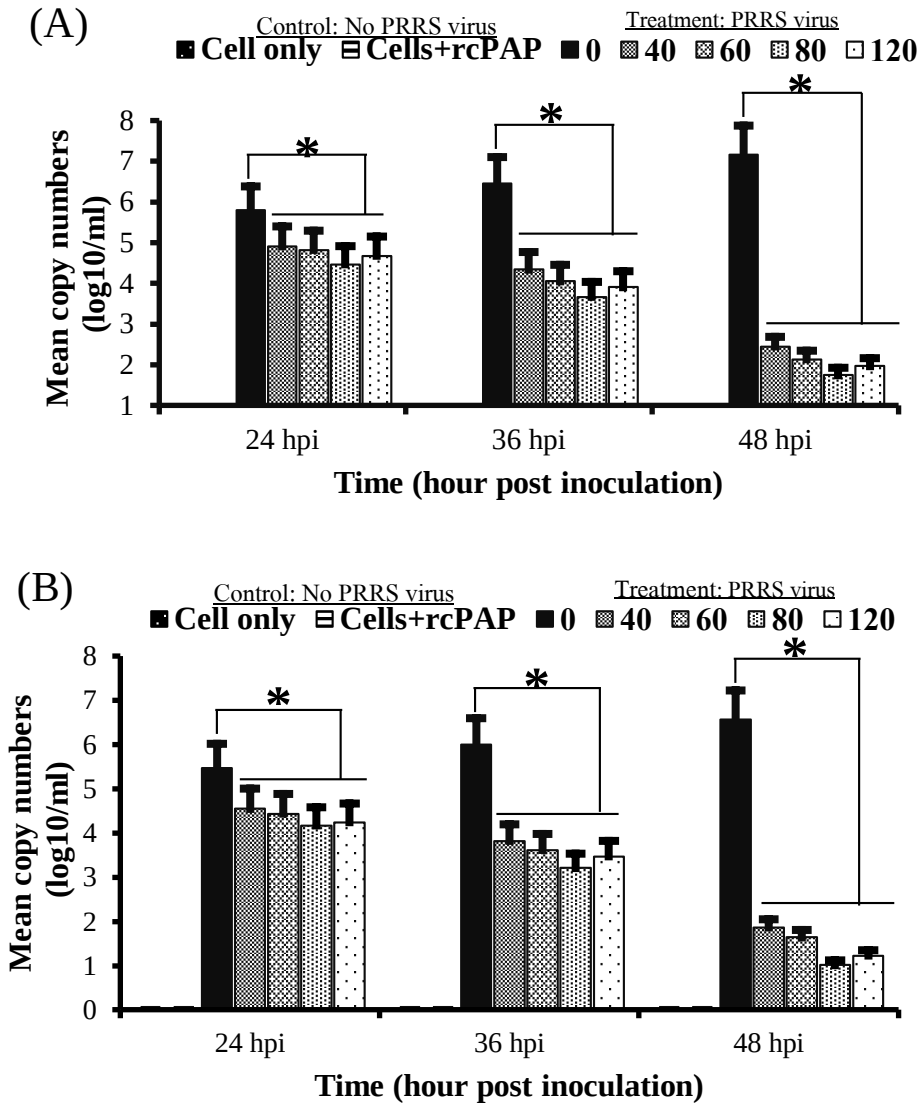


**Figure 4** The enhanced antiviral effects of the rcPAP (μg/ml) treated PRRS virus-infected MARC-145 cells at three time points in (A) culture cells and (B) culture supernatants were performed using qRT-PCR. Data are shown as mean ± SD of six independent experiments. Bars represent the standard deviation. The $p < 0.05$ (*).

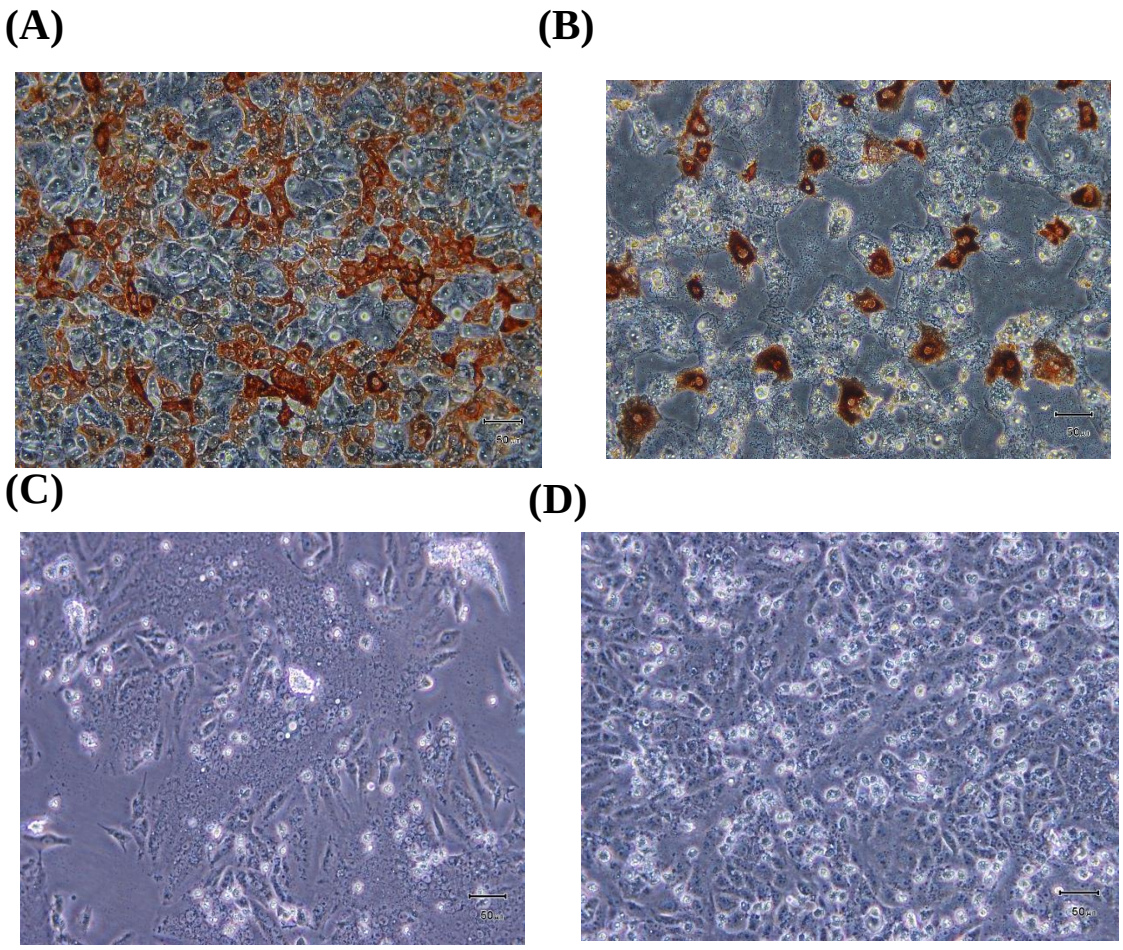


**Figure 5** The PRRS virus and PED alpha-coronavirus induced CPE in culture cells. MARC-145 cells were infected with PRRS virus (200 TCID50 per well) for 48 hpi. Vero cells were infected with PED virus (400 TCID50 per well) for 48 hpi. (A) PRRS virus infection without rcPAP and (B) PRRS virus infection with 80 µg/ml of rcPAP at 48 hpi; (C) PED alpha-coronavirus infection without rcPAP and (D) PED alpha-coronavirus infection with 80 µg/ml of rcPAP at 48 hpi.

In addition, the reduction of viral loads of the rcPAP against PRRS virus was determined. It showed that viral titers were significantly reduced in rcPAP (40, 60, 80 and 120 µg/ml) treated PRRS virus-infected MARC-145 cells ($p < 0.05$) at three different time points (24, 36 and 48 hpi). As shown in Fig. 6A, the highest reduction of viral titers produced by the rcPAP-treated PRRS virus-infected MARC-145 cells at a concentration of 80 µg/ml compared with untreated PRRS virus-infected cells were 59.43% (1.57 ± 0.005 vs 3.87 ± 0.001 log10 ($TCID_{50}$/ml)), 63.13% (1.65 ± 0.006 vs 4.34 ± 0.001 log10 ($TCID_{50}$/ml)) and 87.76% (0.63 ± 0.004 vs 5.15 ± 0.001 log10 ($TCID_{50}$/ml)) at 24, 36 and 48 hpi, respectively ($p<0.05$). In this experiment, the results clearly demonstrated that rcPAP at a concentration of 80 µg/ml significantly reduced by 87.76% of PRRS viral titers at 48 hpi compared with untreated controls ($p < 0.05$). The correlation between methods of qRT-PCR and viral titration in this study showed strong and positive linear relationship with r = 0.972 values as shown in Fig. 11A. Both validated methods to confirm the enhanced the viral load reduction efficacy can be used in this study.

To further validate the results obtained from qRT-PCR and viral titers, Western blot analysis of virus-infected cell lines was detected the PRRS viral N protein band (15 kDa) at 24 hpi (Fig. 7A) and 36 hpi (Fig. 7B) but was not detected at 48 hpi (Fig. 7C). Viral N protein synthesis was decreased when adding at high concentration of rcPAP (80 and 120 µg/ml) in PRRS virus-infected MARC-145 cells at 36 hpi and was not detected at 48 hpi compared with untreated infected cells due to the reduction of viral propagation.

***PED alpha-coronavirus infected Vero cells:*** As shown in Fig. 8, the untreated PED alpha-coronavirus infected Vero cells at 48 hpi had numbers of viral RNA reaching the value of 7.73 ± 0.004 log10 (copies/ml). As expected, the administration of the rcPAP significantly reduced the copy numbers of PED alpha-coronavirus RNA in culture cells (Fig. 8A) and supernatants (Fig. 8B) at three different-time points (24, 36 and 48 hpi) ($p < 0.05$). In Fig. 8A, the highest reduction of intracellular viral RNA in rcPAP-treated PED alpha-coronavirus infected Vero cells at a concentration of 80 µg/ml was 19.83% (4.97 ± 0.005 vs 6.28 ± 0.001 log10 (copies/ml)), 41.78% (4.11 ± 0.001 vs 7.06 ± 0.008 log10 (copies/ml)) and 74.38 % (1.98 ± 0.01 vs 7.73 ± 0.004 log10 (copies/ml)) compared with untreated Thai isolated PED alpha-coronavirus infected Vero cells at 24, 36 and 48 hpi, respectively ($p < 0.05$). In culture supernatants as shown Fig. 8B, we observed that the highest reduction of viral copy numbers in rcPAP-treated PED alpha-coronavirus infected Vero cells at a concentration of 80 µg/ml were 21.31% (4.43 ± 0.005 vs 5.63 ± 0.003 log10 (copies/ml)), 44.91% (3.36 ± 0.002 vs

6.1 ± 0.001 log10 (copies/ml)) and 82.98 % (1.14 ± 0.004 vs 6.74 ± 0.001 log10 (copies/ml)) at 24, 36 and 48 hpi, respectively, compared with untreated Thai isolated PED alpha-coronavirus infected Vero cells ($p < 0.05$). This observation clearly indicates that rcPAP (80 µg/ml) treated Thai isolated PED alpha-coronavirus infected Vero cells were significantly reduced up to 74.38% and 82.98% in culture cells and supernatants, respectively, at 48 hpi ($p < 0.05$) as taking pictures under the inverted microscope shows in Figs. 5C (without rcPAP) and D (with rcPAP).

Furthermore, we found that the mean PED alpha-coronavirus titers on culture supernatants produced by rcPAP (40, 60, 80 and 120 µg/ml) treated with PED alpha-coronavirus infected Vero cells (Fig. 6B) were significantly reduced compared with untreated PED alpha-coronavirus infected Vero cells at three different-time points (24, 36 and 48 hpi) ($p < 0.05$). The highest reduction of viral loads when using the rcPAP at a concentration of 80 µg/ml were 58.04% (1.72 ± 0.002 vs 4.13 ± 0.001 log10 (TCID50/ml)), 61.95% (1.75 ± 0.002 vs 4.64 ± 0.001 log10 (TCID50/ml)) and 86.29% (0.74 ± 0.002 vs 5.47 ± 0.002 log10 (TCID50/ml)) at 24, 36 and 48 hpi, respectively. The correlation between methods of qRT-PCR and viral titration in this study showed strong and positive linear relationship with r = 0.976 values as shown in Fig. 11B. Both validated methods confirm the enhanced the viral load reduction efficacy can be used in this study.

The Western blot results showed the reduction of PED alpha-coronavirus N protein bands (58 kDa) in culture cells after being treated with rcPAP (80 and 120 µg/ml) at 24 hpi (Fig. 9A) and 36 hpi (Fig. 9B). Interestingly, the PED alpha-coronavirus N protein bands were not detected at 48 hpi (Fig. 9C).

***Apoptosis assay:*** To examine the rcPAP induced apoptosis in PRRS virus-infected MARC-145 cells or PED alpha-coronavirus infected Vero cells during the early phase of infection, monkey active caspase-3 levels were detected using ELISA analysis. As shown in Fig. 10A, the levels of monkey active caspase-3 in rcPAP (40, 60, 80 and 120 µg/ml) treating PRRS virus-infected MARC-145 cells were significantly increased in a dose-dependent manner compared to untreated PRRS virus-infected cells (positive control) at different time points (24, 36 and 48 hpi) ($p < 0.05$), respectively. The results indicate that the highest monkey active caspase-3 levels in rcPAP (80 µg/ml) treated PRRS virus-infected MARC-145 cells were 12.69 fold (6.73 ± 0.008 vs 0.53 ± 0.003 (ng/mg protein)), 14.18 fold (9.08 ± 0.003 vs 0.64 ± 0.002 and (ng/mg protein)) 17.9 fold (9.15 ± 0.008 vs 0.51 ± 0.003 (ng/mg protein)) at 24, 36 and 48 hpi, respectively, compared with untreated control. From our results, the highest concentration of monkey active caspase-3 levels was 13.36 ng/mg protein at a concentration of 80 µg/ml of rcPAP treating PRRS virus-infected MARC-145 cells for 48 hpi. Similar results were observed in rcPAP treated Thai isolated PED alpha-coronavirus infected Vero cells (Fig. 10B). The results showed that the highest monkey active caspase-3 levels in rcPAP (80 µg/ml) treated Thai isolated PED alpha-coronavirus infected Vero cells were 12.08 fold (6.89 ± 0.001 vs 0.57 ± 0.003 (ng/mg protein)), 14 fold (8.54 ± 0.003 vs 0.61 ± 0.004 (ng/mg protein)) and 15.49 fold (10.07 ± 0.006 vs 0.65 ± 0.001 (ng/mg protein)) at 24, 36 and 48 hpi, respectively, compared with the untreated control. In the rcPAP treated PED alpha-coronavirus infected cells, the highest concentration of monkey active caspase-3 levels was 13.17 ng/mg protein at a concentration of 80 µg/ml at 48 hpi compared with the untreated control. This data shows that rcPAP have induced apoptosis in either PRRS virus-infected MARC-145 cells or PED alpha-coronavirus infected Vero cells.

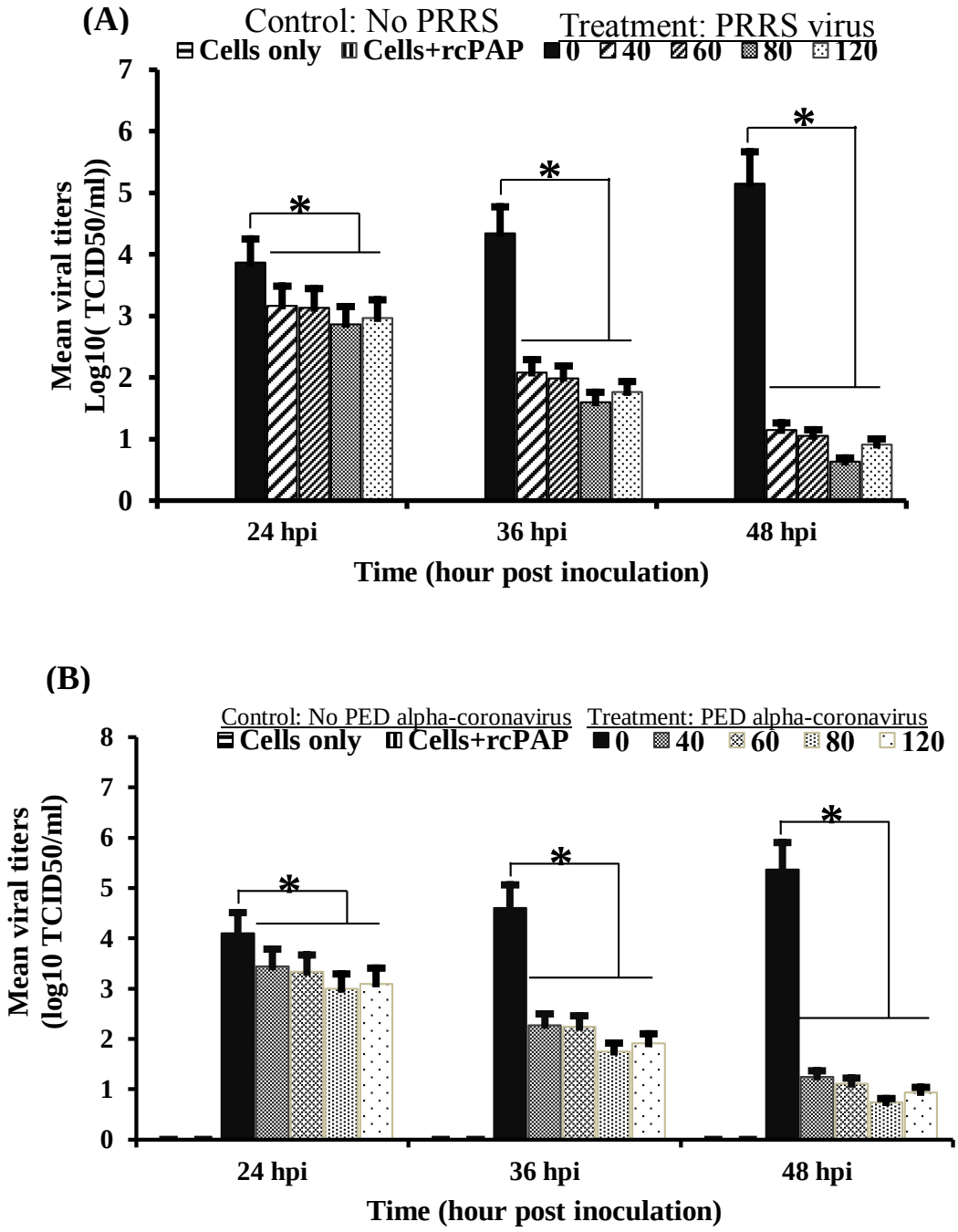


**Figure 6** Mean viral titers in culture supernatants of the rcPAP (µg/ml) treated (A) PRRS virus-infected MARC-145 cells and (B) PED alpha-coronavirus infected Vero cells at three-time points, respectively. Titers are expressed as log10 TCID50 per ml of six independent experiments. Bars represent the standard deviation. The $p < 0.05$ (*).

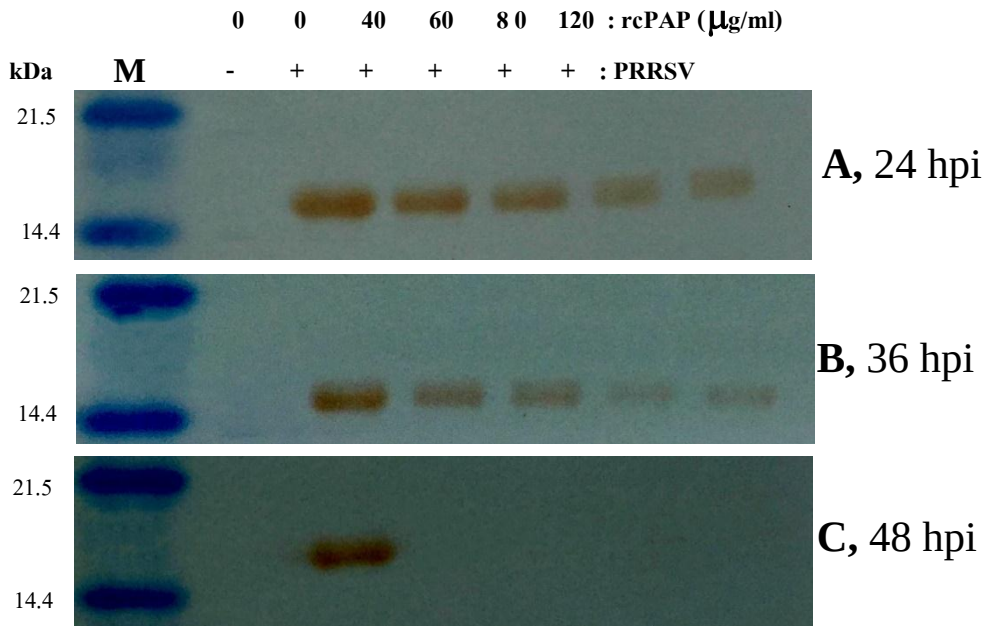


**Figure 7** The band patterns of PRRS virus N protein was analyzed by Western blot after treatment with the rcPAP (mg/ml) at the indicated concentrations or PBS for (A) 24 hpi, (B) 36 hpi and (C) 48 hpi, respectively. M, Protein markers. Protein markers (BioRad) on the gels are indicated in kDa.

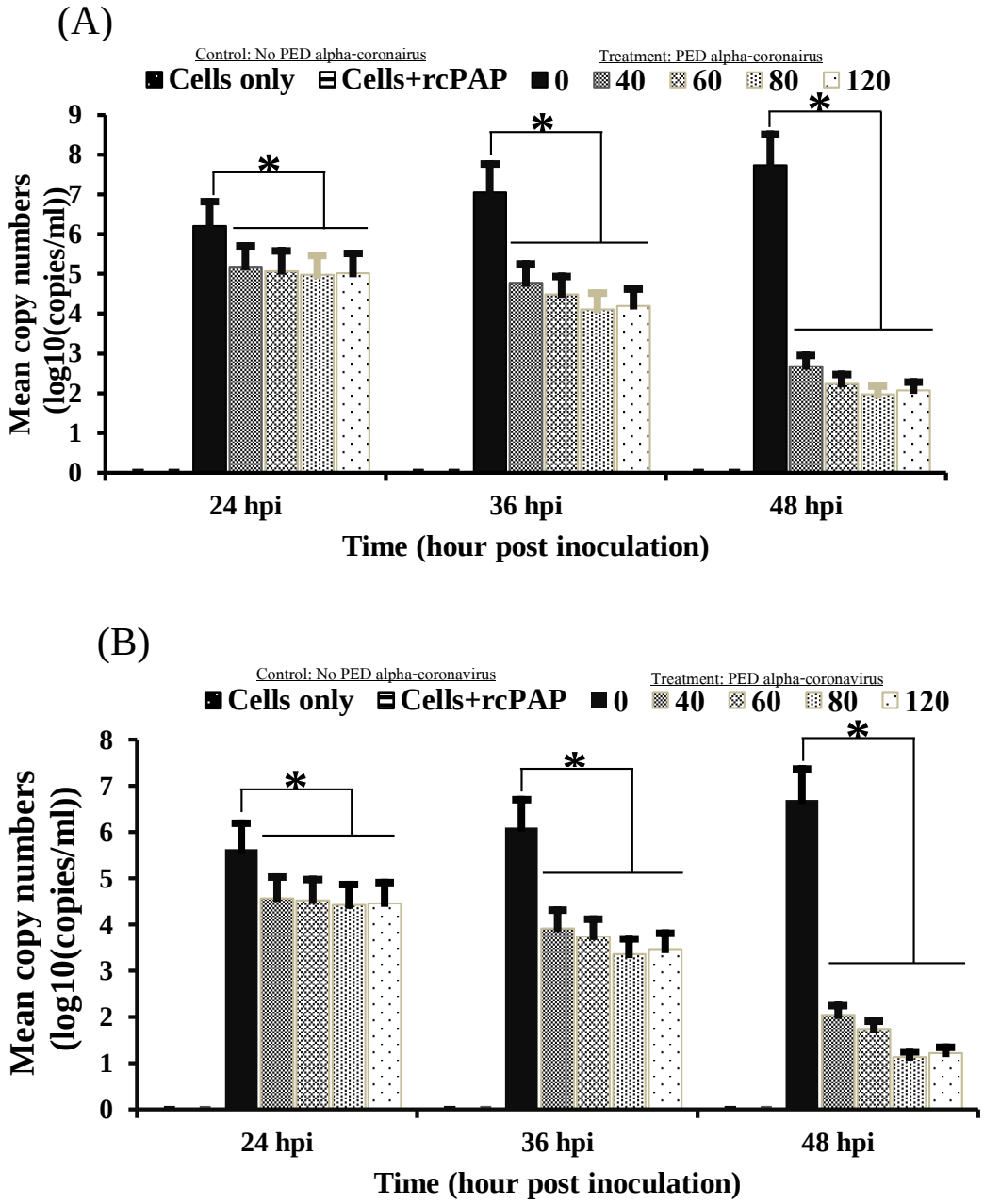


**Figure 8** The enhanced antiviral effects of the rcPAP (μg/ml) treated PED alpha-coronavirus infected Vero cells at three-time points in (A) culture cells and (B) culture supernatants were performed using qRT-PCR. Data is shown as mean ± SD of six independent experiments. Bars represent the standard deviation. The $p < 0.05$ (*).

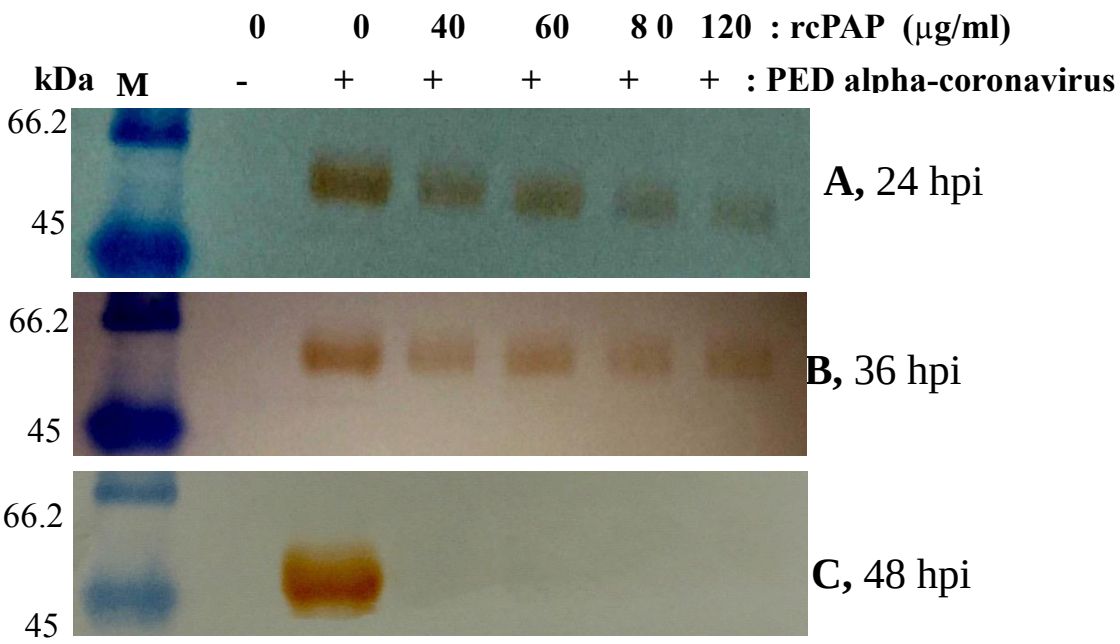


**Figure 9** The banding pattern of PED alpha-coronavirus N protein was analyzed by western blot after treatment with the rcPAP (μg/ml) at the indicated concentrations or PBS for (A) 24 hpi, (B) 36 hpi and (C) 48 hpi, respectively. M, Protein markers. Protein markers (BioRad) on the gels are indicated in kDa.

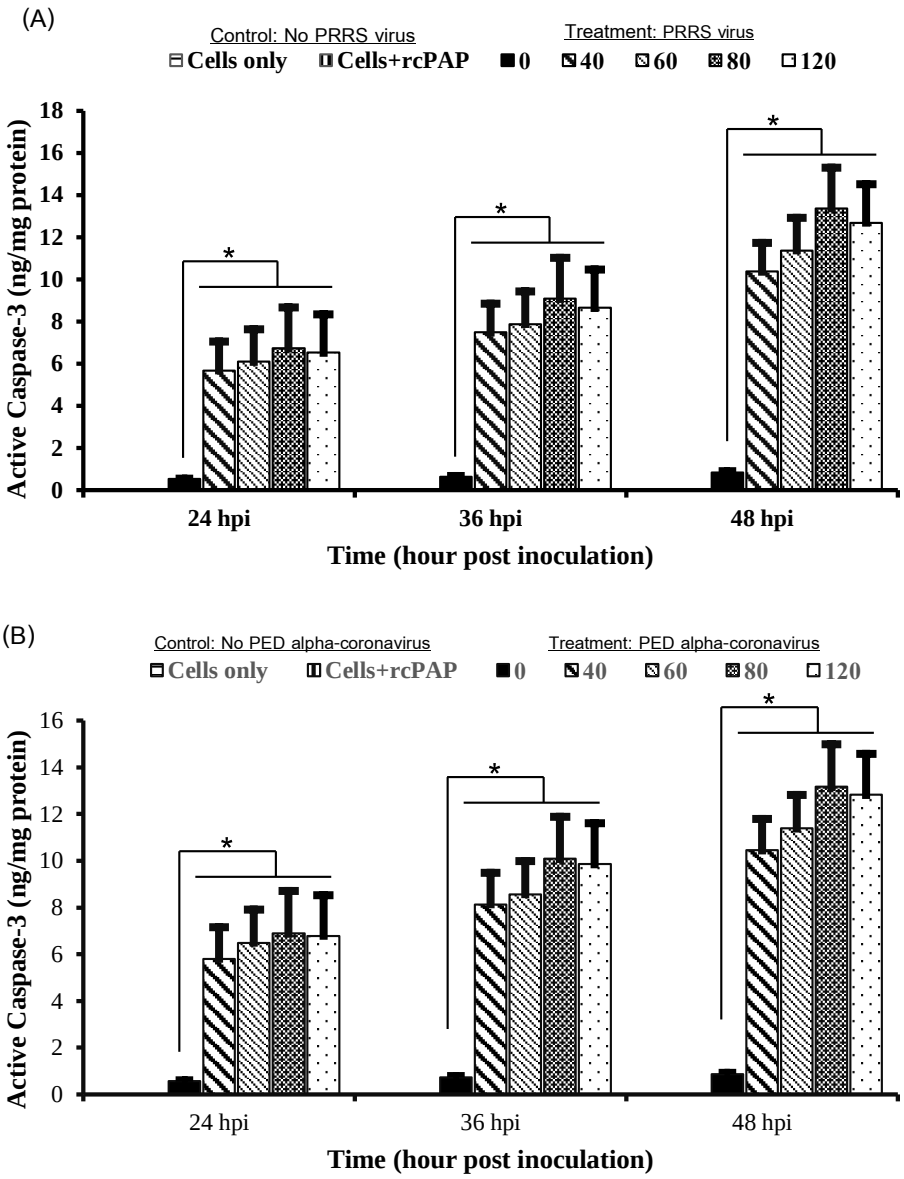


**Figure 10** The monkey active caspase-3 levels in (A) MARC-145 culture cells and (B) Vero culture, cells were measured via ELISA technique and measured the protein concentration. Data are shown as mean ± SD of six independent experiments. Bars represent the standard deviation. The $p < 0.05$ (*).

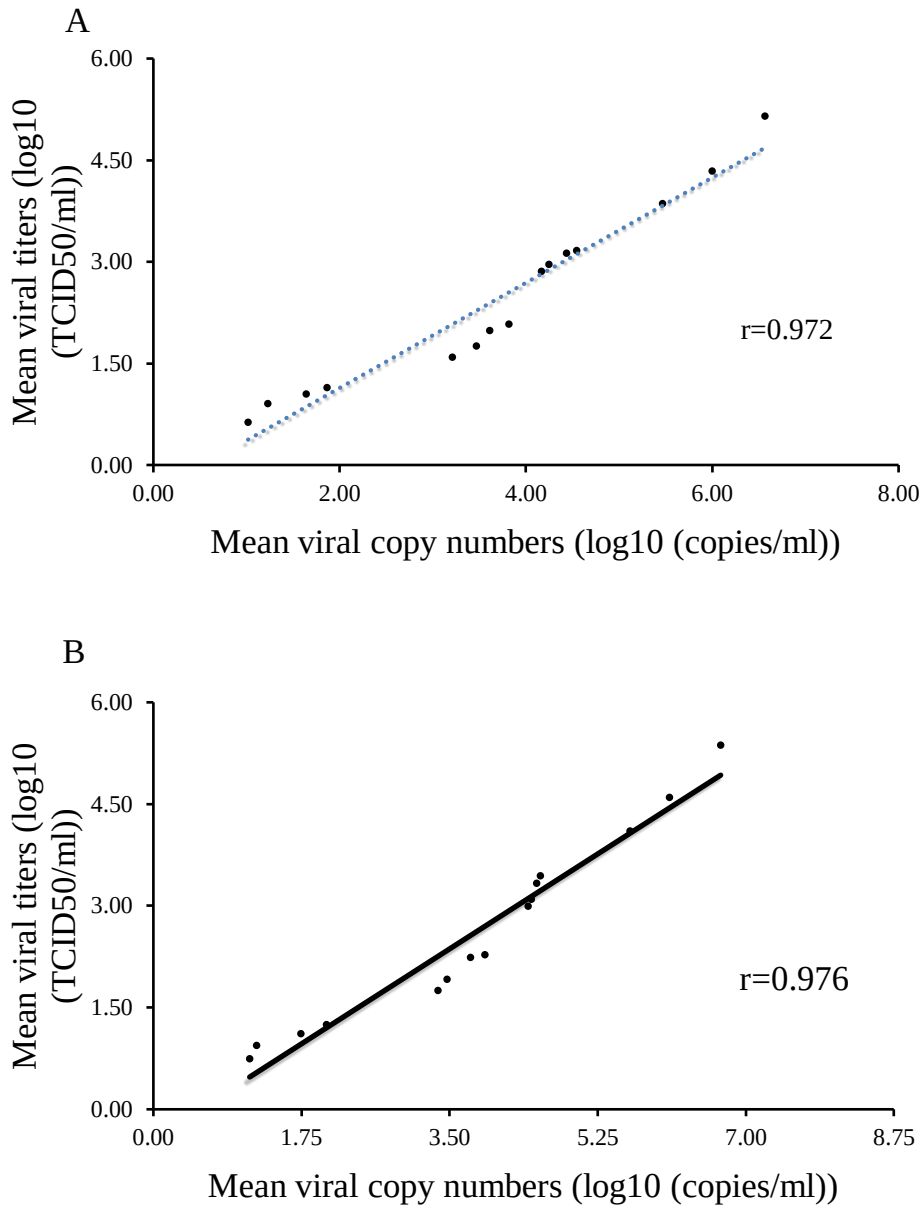


**Figure 11** The correlation between methods of qRT-PCR (log10 (copies/ml) and viral titers (log10 ($TCID_{50}$/ml) in (A) PRRS virus-infected MARC-145 cells and (B) PED alpha-coronavirus infected Vero cells.

## *Discussion*

The high prevalence and the limited efficacy of both inactivated and MLV vaccines of PRRS virus and PED alpha-coronavirus have shown the necessity to search for effective antiviral drugs or molecules. The DRACO molecule, as a novel concept, specifically targets the virus-infected cells and displays highly biological stability. The DRACO molecule in humans and in pigs has been reported to be used to control the viral diseases *in vitro* (Rider *et al*., 2011, Guo *et al*., 2015). These two pathways (interferon and apoptosis) originated from the idea that the human DRACO concept can be combined to circumvent most viral blockades including two major swine positive-strand RNA viruses such as PRRS virus and PED alpha-coronavirus. This study is the first report that rcPAP, which combines two pathways (interferon and apoptosis) originated from the human DRACO concept, produced from bacteria that is a chimeric protein derived from swine PKR and swine Apaf-1 induced cell death and enhanced viral load reduction activity against PRRS virus and PED alpha-coronavirus using two cell lines, MARC-145 and Vero cells. The reducing viral-load efficacy of rcPAP against both viruses appears to be more species-specific. Not only do most of the ideal antiviral molecules inhibit the synthesis of virus or stimulate host-encoded elements in controlling virus growth but also our rcPAP can have the biological effect to reduce the virus-infected cell lines as well.

In this study, the HIV TAT domain as protein transduction domain (PTD) part was successfully fused with our rcPAP and showed the effect of delivering the rcPAP into either MARC-145 or Vero cells as previously reported by Guo *et al*. (2015), and Zhang *et al*. (2013), (Zhang *et al*., 2013, Guo *et al*., 2015). The HIV TAT domain may have transduced rcPAP into MARC-145 and Vero cells via macropinocytosis as previously reported (Murriel and Dowdy 2006). The transduction effect using the Western blot technique clearly demonstrated that the rcPAP got into and was

inside both MARC-145 cells and Vero cells and persisted for at least 3 days. Interestingly, previous studies by Rider *et al*. (2011), showed the persisting time of a human DRACO molecule for at least 8 days (Rider *et al*., 2011). Further investigation needs to address the maximum times that rcPAP can persist inside the cells and still have antiviral activity.

This study also indicated that the concentration of rcPAP at 40, 60 and 80 µg/ml was not toxic, both of these normal cell lines using MTT assay and Trypan blue assay. However, at a concentration of 120 µg/ml, rcPAP showed a few reductions of cell viability with less than 4.5% by using both assays. Human DRACO molecules produced by bacteria (5 to 20 µg/ml) also reported no toxicity in 11 studied cell lines by Rider *et al*. (2011), (Rider *et al*., 2011). Compared with the DRACO molecule in pigs produced by bacteria (Guo *et al*., 2015) at a concentration of 120 µg/ml showed very high cytotoxicity in the reduction of cell viability in more than 80% in MARC-145 cell lines. One explanation for this may be that the purified processes to reduce contamination with toxin are important steps. The purified rcPAP was dialyzed against PBS buffer overnight to remove *E. coli* toxin (Vo *et al*., 2020). We observed that at a concentration of 120 µg/ml, our rcPAP was less toxic to Vero cells (3.6 ± 0.006%) than MARC-145 cells (4.3 ± 0.009%) even though both cell lines are monkey kidney cell lines. However, observation of cytotoxicity of rcPAP on swine cell line and primary cell origin and the reduction of bacterial toxin using antitoxin absorbent column needs to be further studied.

The dsRBD of swine PKR in our rcPAP showed the effect on viral dsRNA detection in virus-infected cells. Previous reports from Weber *et al*., (2006) demonstrated that significant amounts of viral dsRNA can be detected in a range of viruses with a genome consisting of positive-strand RNA, dsRNA, or DNA but not negative-strand RNA viruses (Weber *et al*., 2006). The PRRS virus and PED alpha-coronavirus belong to different families and show similar positive-strand RNA viruses (Lee 2015, OIE 2015). The dsRBD of PKR bind to viral dsRNA in the interferon pathway (Dauber and Wolff 2009). In previous reports, the dsRBD detection of either human PKR in human DRACO or swine PKR in DRACO molecule in pigs (Rider *et al*., 2011, Guo *et al*., 2015) is successfully bound to viral dsRNA in virus-infected cells.

Apoptosis is considered to be an important host-defense mechanism that interrupts viral replication and eliminates virus-infected cells (Koyama *et al*., 2008). The CARD domain of our rcPAP was constructed to induce apoptosis in virus-infected cells. The monkey active caspase-3 levels clearly demonstrated that rcPAP significantly induced apoptosis over the study ($p < 0.05$). To our surprise, the rcPAP molecule (80 µg/ml) was shown the significant effect of inducing the apoptosis protein (monkey active caspase-3) as shown the increase of monkey active caspase-3 by 16.09-fold in PRRS virus-infected MARC-145 cells and 15.49 fold in PED alpha-coronavirus infected cells with rcPAP (80 µ/ml) at 48 hpi ($p < 0.05$) compared with untreated infected control. The studies of Rider *et al*. (2011), and Guo *et al*. (2015), have demonstrated that the CARD domain of Apaf-1 induced apoptosis in virus-infected cells (Rider *et al*., 2011, Guo *et al*., 2015). In agreement with those studies, the rcPAP can induce apoptosis on PRRS virus-infected MARC-145 cells and on PED alpha-coronavirus infected Vero cells via activation of caspase 9 (caspase 9 is an initiator caspase in the intrinsic apoptotic pathway (Elmore 2007)). Once activated, active caspase 9 activates caspase 3 (caspase 3 is the key protease activated during early apoptosis as the apoptotic marker (Elmore 2007)). The monkey active caspase-3 levels were undetermined from both two negative controls (one cell with rcPAP and other cells without rcPAP). It implies that our rcPAP did not induce apoptosis in normal cells (viral dsRNA are not present). We could infer that three parts in our molecules had successfully done their work on virus-infected cells.

A time course study revealed that rcPAP showed the reduction of viral replication when it was added after the PRRS virus and PED alpha-coronavirus entered the cell line. For the rcPAP efficacy of PRRS virus, the enhanced reducing viral-load activity against PRRS virus-infected MARC-145 cells (200 TCID50) clearly showed that at a concentration of 80 µg/ml of rcPAP significantly reduced PRRS virus copy numbers (84.47%) and viral titers (87.76%) ($p < 0.05$) at 48 hpi compared with untreated infected control, indicating enhanced antiviral activity of rcPAP against PRRS virus, likely accomplished through killing PRRS virus-infected cells. In comparison with previous reports by Li *et al*. (2015), using miRNAs (Liwei *et al*., 2015) and Li *et al*. (2015), using siRNAs (Li *et al*., 2015) significantly showed the suppression of PRRS virus RNA copy numbers (about 40%) and viral titers (about 60%) by directly targeting the viral genome. It is likely that apoptosis induction of rcPAP on virus-infected was responsible for the reduction of PRRS virus genomic RNA and titers. To our knowledge, rcPAP did not destroy viral particles or directly inhibit viral replication by target viral genome instead of indirectly via apoptosis induction to kill virus-infected cells. However, at a concentration of 120 µg/ml of rcPAP showed less the reducing viral-load activity than that of at 80 µg/ml. These results may be related to the cytotoxicity of rcPAP. Although the rcPAP was added to infected cell lines after viral inoculation, further study will address the different administration times of rcPAP such as before or together with viral inoculation.

The PRRS virus N protein, the most abundant viral protein expressed in infected cells, blocks host protein synthesis due to its high concentration in the nucleolus (Jourdan *et al*., 2012). Moreover, the PRRS virus N protein may affect transcriptional regulation in infected cells by interacting with transcriptional regulators (Dokland 2010). Here, we showed that the rcPAP effectively decreased the PRRS virus-infected MARC-145 cells. Theoretically, our rcPAP did not directly inhibit viral protein synthesis. The reduction of viral N protein in rcPAP treated virus-infected cells may be related to the apoptosis induction of rcPAP to kill virus-infected cells. However, we do not have data to support this theory since the viral N gene expression was not monitored and its role in PRRS virus replication is not well understood. It implies that

rcPAP may reduce PRRS viral-infectious clones and viral loads.

For PED alpha-coronavirus, we studied the reducing viral-load activity of the rcPAP against 400 TCID50 (general use of 200 TCID50/well) of the PED alpha-coronavirus to infect Vero cells. In addition, the results also indicated that our rcPAP at a concentration of 80 µg/ml significantly reduced both PED alpha-coronavirus copy numbers (82.98%) and viral titers (86.19%) ($p < 0.05$) against high 400 TCID50 of PED alpha-coronavirus infected cells compared with untreated infected cells at 48 hpi. Our study had better results than the study by Kwon *et al*. (2013), (Kwon *et al*., 2013) that has shown the reduction of viral copy numbers (from 30% to 40%) by inhibition both PED alpha-coronavirus entry and replication via inhibition of viral RNA and protein synthesis in Vero cells treated with phlorotannins extracted from herbs. Recently, the study of Li *et al*.(2019), (Li *et al*., 2019) showed that Grifthsin could reduce PEDV infection of Vero cells by about 82.8% by preventing viral attachment to host cells and disrupting cell-to-cell transmission. However, the effect of the added times of rcPAP on Vero cells, such as before or together with PED alpha-coronavirus infection needs to be further studied. In our study, four concentrations of rcPAP (40, 60, 80 and 120 µg/ml) were tested and showed that rcPAP at a concentration of 80 µg/ml significantly reduced more PED alpha-coronavirus than those of other concentrations at 48 hpi ($p < 0.05$).

The PED alpha corona viral N protein is a phosphorylated structural protein that is associated with the viral genome and is abundant in virus-infected cells (Li *et al*., 2013). Therefore, the appearance of the N protein indicates replication of PED alpha-coronavirus and this can be used for early and accurate detection of virus replication in infected cells (Li *et al*., 2013). The PED alpha-coronavirus N protein has multiple functions in viral replication and pathogenesis and also disturbs antiviral responses by antagonizing interferon production (Lee 2015). We observed lower PED alpha-coronavirus N protein synthesis in the rcPAP treated PED alpha-coronavirus infected Vero cells compared with untreated PED alpha-coronavirus infected Vero cells at 24 hpi and 36 hpi and not detect at 48 hpi. As expected, the rcPAP may effectively interact with infected Vero cells with PED alpha-coronavirus propagation. Consistent with the recent study of porcine viperin can inhibit the proliferation of PED alpha-coronavirus in IPEC-J2 cells (Wu *et al*., 2020).

Taken together, rcPAP at a concentration of 80 µg/ml significantly showed the maximum enhanced reducing viral-load activity (reduced viral copy numbers, viral titers, viral N protein by induction of apoptosis) in PRRS and PED alpha-coronavirus infected cell lines at 48 hpi ($p<0.05$). These results will encourage us to further investigate the in vivo effect of a rcPAP on the reduction of viral shedding in nursery pigs after vaccination with PRRS MLV vaccine. For PED alpha-coronavirus, however, further study is needed to investigate the in vivo efficacy of rcPAP on day 1 to day 3 of newborn piglets.

In conclusion, the data included in this report provides that the rcPAP produced from the bacterial system exhibits strong reducing viral-load activity via apoptosis induction against both PRRS virus and PED alpha-coronavirus in cell lines. The rcPAP may be used in the development of prophylactic and therapeutic strategies for these two diseases and other viral diseases in swine. However, the enhanced reducing viral-load efficacy of the rcPAP needs further confirmation *in vivo.*

## *Acknowledgements*

We would like to thank Chulalongkorn University for providing scholarships to Phong Vu Anh Tuan Vo.

## *References*

Abba Y, Hassim H, Hamzah H and Noordin MM 2015. Antiviral Activity of Resveratrol against Human and Animal Viruses. Advances in Virology. 2015: 1-8.

Billack B, Radkar V and Adiabouah C 2008. In vitro evaluation of the cytotoxic and antiproliferative properties of resveratrol and several of its analogs. Cell Mol Biol Lett. 13: 553-569.

Borel N, Dumrese C, Ziegler U, Schifferli A, Kaiser C and Pospischil A 2010. Mixed infections with Chlamydia and porcine epidemic diarrhea virus - a new in vitro model of chlamydial persistence. BMC Microbiology. 10: 1-9.

Choi H, Kim J, Lee C, Ahn Y, Song J, Baek S and Kwon D 2009. Antiviral activity of quercetin 7-rhamnoside against porcine epidemic diarrhea virus. Antiviral Research. 81: 77-81.

Dauber B and Wolff T 2009. Activation of the Antiviral Kinase PKR and Viral Countermeasures. Viruses. 1: 523-544.

Ding X, Xu F, Chen H, Tesh RB and Xiao S 2005. Apoptosis of Hepatocytes Caused by Punta Toro Virus (Bunyaviridae: Phlebovirus) and Its Implication for Phlebovirus Pathogenesis. Am J Pathol. 167: 1043-1049.

Dokland T 2010. The structural biology of PRRSV. Virus Res. 154: 86-97.

Elmore S 2007. Apoptosis: A Review of Programmed Cell Death. Toxicol Pathol. 35: 495-516.

Guo C, Chen L, Mo D, Chen Y and Liu X 2015. DRACO inhibits porcine reproductive and respiratory syndrome virus replication in vitro. Arch Virol. 160: 1-9.

Jourdan SS, Osorio FA and Hiscox JA 2012. Biophysical characterisation of the nucleocapsid protein from a highly pathogenic porcine reproductive and respiratory syndrome virus strain. Biochem Biophys Res Commun. 419: 137-141.

Koyama S, Ishii KJ, Coban C and Akira S 2008. Innate immune response to viral infection. Cytokine. 43: 336-341.

Kwon H, Ryu YB, Kim Y, Song N, Kim CY, Rho M, Jeong J, Cho K, Lee WS and Park S 2013. In vitro antiviral activity of phlorotannins isolated from Ecklonia cava against porcine epidemic diarrhea coronavirus infection and hemagglutination. Bioorg Med Chem. 21: 4706-4713.

Lee C 2015. Porcine epidemic diarrhea virus: An emerging and re-emerging epizootic swine virus. Virol J. 12: 1-16.

Li L, Wei Z, Zhou Y, Gao F, Jiang Y, Yu L, Zheng H, Tong W, Yang S, Zheng H, Shan T, Liu F, Xia T and Tong G 2015. Host miR-26a suppresses replication of porcine reproductive and respiratory syndrome virus by upregulating type I interferons. Virus Res. 195: 86-94.

Li L, Yu X, Zhang H, Cheng H, Hou L, Zheng Q and Hou J 2019. In vitro antiviral activity of Grifthsin against porcine epidemic diarrhea virus. Virus Genes. 55: 174-181.

Li z, Chen F, Yuan Y, Zeng X, Wei Z, Zhu L, Sun B, Xie Q, Cao Y, Xue C, Ma J and Bee Y 2013. Sequence and phylogenetic analysis of nucleocapsid genes of porcine epidemic diarrhea virus (PEDV) strains in China. Arch Virol. 158: 1267-1273.

Liwei L, Gao F, Jiang Y, Yu L, Zhou Y, Zheng H, Tong W, Yang S, Xia T, Qu Z and Tong G 2015. Cellular miR-130b inhibits replication of porcine reproductive and respiratory syndrome virus in vitro and in vivo. Sci Rep: 1-10.

Ma Z, Wang Y, Zhao H, Xu A, Wang Y, Tang J and Feng W 2013. Porcine Reproductive and Respiratory Syndrome Virus Nonstructural Protein 4 Induces Apoptosis Dependent on Its 3C-Like Serine Protease Activity. PLoS ONE. 8: 1-11.

Miller LC, Crawford KK, Lager KM, Kellner SG and Brockmeier SL 2016. Evaluation of two real-time polymerase chain reaction assays for Porcine epidemic diarrhea virus (PEDV) to assess PEDV transmission in growing pigs. J Of Veterinary Diagnostic Investigation. 16: 20-19.

Mojtaba Sharti M, Ghaleh HEG, Kondori BJ and Dorostkar R 2021. Double-stranded RNA Activated Caspase Oligomerizer (DRACO): Designing, Subcloning, and Antiviral Investigation. J Appl Biotechnol Rep. 8(1): 46-50.

Murriel CL and Dowdy SF 2006. Influence of protein transduction domains on intracellular delivery of macromolecules. Expert Opin Drug Deliv. 3: 1-8.

OIE 2015. Porcine reproductive and respiratory syndrome. Terrestrial manual: 1-13.

Pozzo FD and Thiry E 2014. Antiviral chemotherapy in veterinary medicine: current applications and perspectives. Rev Sci Tech Off Int Epiz. 33: 1-27.

Quinn PJ, Markey BK, Leonard FC, FitzPatrick ES and Fanning S 2015. Concise Review of Veterinary Microbiolog. 2nd edition ed. Wiley Blackwell: 208 pp.

Reed LJ and Muench H 1938. A simple method of estimating fifty percent endpoints. Am J Epidemiol. 27.

Rider TH, Zook CE, Boettcher TL, Wick ST, Pancoast JS and Zusman BD 2011. Broad-Spectrum Antiviral Therapeutics. PLOS ONE. 6: 1-15.

Song D, Moon H and Kang B 2015. Porcine epidemic diarrhea: a review of current epidemiology and available vaccines. Clin Exp Vaccine Res. 4: 166-176.

Tatsanakit A, Kesdangsakonwut S and Thanawongnuwech R 2003. Evaluation of monoclonal antibodies for PRRSV detection of the selected Thai isolated using immunoperoxidase monolayer assay (IPMA). 11th International Symposium of the World Association of Veterinary laboratory Diagnosticians and OIE seminar on biotechnology.

Uma S, Kelly JP and Rajasekaran SK 2008. An investigation of the value of the Tetrahymena pyriformis as a test organism for assessing the acute toxicity of antidepressants. Biomed Res. 19: 37-40.

Valiyari S, Baradaran B, Delazar A, Pasdaran A and Zare F 2012. Dichloromethane and Methanol Extracts of Scrophularia oxysepala Induces Apoptosis in MCF-7 Human Breast Cancer Cells. Adv Pharm Bull. 2: 223-231.

Vo PVAT, Leksakchai T, Kedkovid R, Tawatsin A and Nuntaprasert A 2020. Production of recombinant chimeric swine PKR-APAF-1 protein and its apoptotic induction on MARC-145 cells. Thai J. Vet. Med. 50: 137-148.

Wardi L, Alaaeddine N, Raad I, Sarkis R, Serhal R, Khalil C and Hilal G 2014. Glucose restriction decreases telomerase activity and enhances its inhibitor response on breast cancer cells: possible extra-telomerase role of BIBR 1532. Cancer Cell International. 60: 1-14.

Weber F, Wagner V, Rasmussen SB, Hartmann R and Paludan SR 2006. Double-Stranded RNA Is Produced by Positive-Strand RNA Viruses and DNA Viruses but Not in Detectable Amounts by Negative-Strand RNA Viruses. J VIROL. 80: 5059–5064.

Wernike K, Hoffmann B, Dauber M, Lange E, Schirrmeier H and Beer M 2012. Detection and Typing of Highly Pathogenic Porcine Reproductive and Respiratory Syndrome Virus by Multiplex Real-Time RT-PCR. PLoS ONE. 7: 1-9.

Zhang X, He D, Zhou B, Pang R, Liu K, Zhao J and Chen P 2013. In vitro inhibition of vesicular stomatitis virus replication by purified porcine Mx1 protein fused to HIV-1 Tat protein transduction domain (PTD). Antiviral Research. 99: 149-157.